2015

Chemical quantification with ubiquitous optoelectronic devices

Altamash Mukhtar Fakki

Department:

CHEMICAL QUANTIFICATION WITH UBIQUITOUS OPTOELECTRONIC DEVICES

by

ALTAMASH MUKHTAR FAKKI

A THESIS

Presented to the Faculty of the Graduate School of the

MISSOURI UNIVERSITY OF SCIENCE AND TECHNOLOGY

In Partial Fulfillment of the Requirements for the Degree

MASTER OF SCIENCE IN COMPUTER ENGINEERING

2015

Approved by

Dr. Chang-Soo Kim, Advisor

Dr. Cheng Hsiao Wu

Dr. Minsu Choi

PUBLICATION THESIS OPTION

This thesis consists of the following articles that will be submitted for publication as follows:

Pages 07 - 18 are intended for submission to IEEE SENSORS JOURNAL. Pages 19 - 37 are intended for submission to SENSORS AND ACTUATORS JOURNAL.

ABSTRACT

Optical sensing in medical diagnosis and chemical analysis using optoelectronic devices is a growing technology since it offers many advantages including real time analysis, remote sensing capability and low cost approach. This thesis demonstrates that an optical sensing platform utilizing optical mouse, the ubiquitous optoelectronic computer peripheral, can be used in quantitative oxygen and pH analysis.

Work in the first paper includes the use of optical mice for fluorescence intensity imaging of commercial oxygen patch. This involves gray color intensity analysis of filtered images to determine the gaseous oxygen level.

In the second paper, the optical mice is used to measure light absorption and reflection of commercial pH test strips. This sensing scheme is based on detecting the colorimetric change in response of pH test strips to different pH values. The linearity and sensitivity was comparable to those of traditional spectrometric measurement.

This novel, cost-effective approach demonstrates potential application of using optical mouse for simultaneous monitoring and imaging of biological or chemical samples. Therefore, quantitative chemical analysis is possible with even very common computer peripheral devices with the aid of commercial sensor strips.

ACKNOWLEDGMENTS

I am extremely thankful to my advisor Dr. Chang-Soo Kim for his support, guidance and knowledge imparted to me. I would also like to thank him for supporting my work with graduate research assistantship.

I wish to express my sincere appreciation to Dr. Cheng-Hsiao Wu and Dr. Minsu Choi for having trust in me for timely completion of this work and serving on my committee.

I also thank my family especially my mother Tasleema Mukhtar Fakki, father Mukhtar Yusuf Fakki, sister Farha Nafis M Fakki, and brother Mushafiq M Fakki for their patience, moral support and encouragement.

Finally, I would like to thank my lab mates and my fellow graduate students who always encouraged me.

TABLE OF CONTENTS

Page

LIST OF ILLUSTRATIONS

SECTION

1. INTRODUCTION

1.1. UBIQUITOUS OPTOELECTRONICS FOR CHEMICAL SENSING

A remote optical measurement technique using optoelectronic devices and image processing technique has received considerable attention for analyzing the biological and chemical properties of samples. This thesis focuses on exploring the feasibility of using optical mouse as a low-cost and ubiquitous sensor platform for oxygen and pH quantification.

1.2. OXYGEN SENSING

Optical oxygen sensors are particularly useful in the area of biological monitoring and chemical analysis because of their potential for remote detection and miniaturization. Optical oxygen sensors are becoming more common in many applications compared to traditional electrode oxygen. The optical oxygen sensor work on the principle that oxygen quenches the luminescence emitted from luminescent dyes that are immobilized in an oxygen permeable membrane [1].

In this research, an attempt is made to use easily accessible optoelectronic devices for sensing oxygen. An optical mouse is used as an oxygen sensor platform to explore the feasibility as an analytical device. Luminescence based optical oxygen measurement is achieved by registering images of a commercial oxygen sensor patch with an image sensor of optical mouse.

A blue light-emitting diode (470 nm peak) was used as light source to excite the luminophore responsive to oxygen [2]. A band pass filter (615 nm peak - FWHM 100 nm) was used to pass the fluorescence emission (600nm peak) from the oxygen patch. This approach enables the optical mouse to be used as a photodetector by capturing 2 dimensional 16x16 pixel gray scale images.

The intensity measured is correlated to oxygen concentration using Stern-Volmer equation as follows:

$$I_o/I=1+Ksv\ [O_2] \qquad (1)$$

$$Ksv = k\ I_o \qquad (2)$$

Where I indicates luminescence intensity in the presence of oxygen (the subscript "o" denotes the absence of oxygen) and $[O_2]$, Ksv, k indicates oxygen concentration, Stern-Volmer constant and quencher rate coefficient, respectively. Figure 1.1 shows that emitted fluorescence light intensity from oxygen patch changes reversely proportional to oxygen concentration, so by measuring emitted light intensity ratio (Io/I) of fluorescence, oxygen concentration is determined.

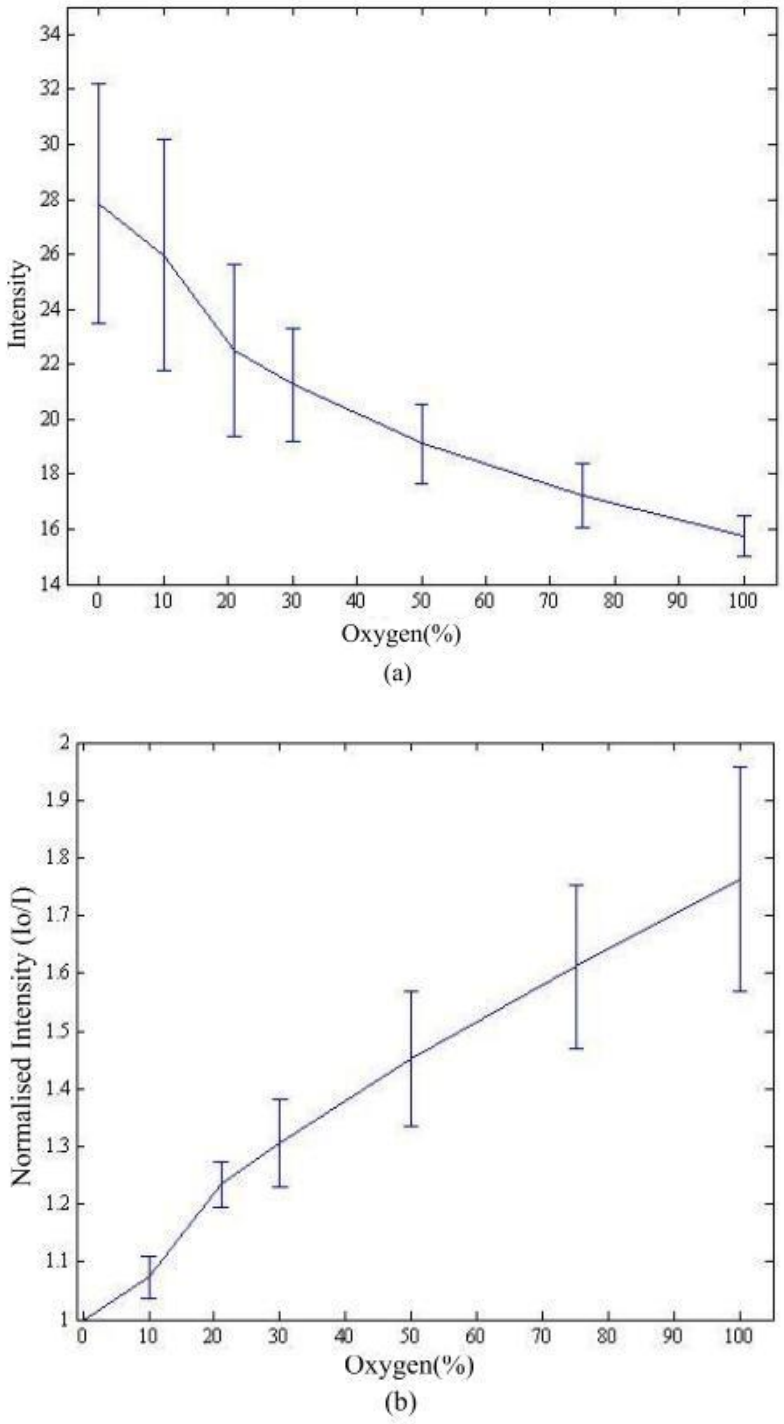

Figure 1.1. Oxygen sensitivity plot using photodetector and blue LED excitation source (a) Intensity vs. oxygen concentration and (b) Stern-Volmer plot

1.3. PH SENSING

Monitoring of pH is required in many chemical reactions, biomedical diagnosis and environment surveillance. Basic principle of a classical pH strips was developed many decades ago [3]. Therefore simple low-cost optoelectronic devices of high stability and high detection sensitivity are in demand and expected to be developed.

An electronic imaging device used in optical mouse is a useful tool for quantitative chemical measurement. Since the image sensor inside optical mouse can detect variation in optical intensities represented by pixels, it is possible to achieve instant two dimensional mapping of multiple colors in gray scale with the help of filters. Therefore we demonstrated novel idea of using optical mouse as colorimetric pH sensor.

Optical pH measurement method based on the color change from dyed cellulose matrix on the commercial Fisherbrand™ laboratory grade plastic pH strips was utilized. Seven pH buffer solutions by FisherScientific™ were selected for wide pH measurement. The pH valuation is based on measuring the reflected light intensity and rate of absorption when there is a change in color of pH indicator covalently immobilized on the cellulose matrix. Thus the pH value of the solution is obtained from the analysis of the registered grayscale images. To verify the proposed grayscale image analysis method, results were compared with those of spectrometric measurements, RGB analysis result and color absorption theory.

Optical effects contribute to convert the pH of the solution into the spectral information [3]. Absorption is the phenomena governing the photons propagating through the optical sensor and determining the intensity and spectral properties of the reflected light. Absorption of light by a pH test strip occurs because the selected frequency of the

illuminated light matches the frequency at which electrons in the atoms of the pH strip material vibrate [4]. If any light that does not have enough or has excessive energy cannot be absorbed is reflected [4].

Figure 1.2 demonstrates the light absorption and reflection as per pH strip color. The information of interest is strictly associated to selective absorption of light by the pH test strip. The color results of the pH strip are in range starts from red (pH2) goes to yellow (pH6), green (pH8) and blue (pH12). A change in color induces a change in the intensities of the reflected light collected by the image sensor. In pH2 the result color is red so it reflects the most of incident red light. This is due to the fact that the red color component absorbs all color light but red light [5]. Whereas pH12 falls in blue color family which absorbs most of red light. Thus, pH value of the solution can be obtained from the analysis of the reflected light emission intensities and red light absorption.

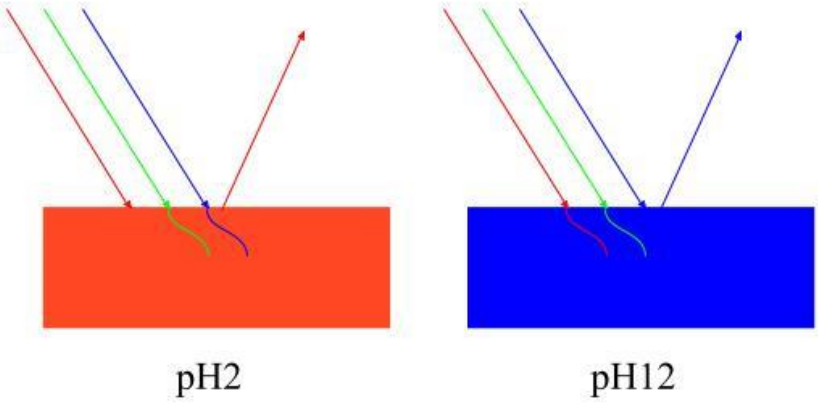

Figure 1.2. Color absorption and reflection of pH test strips in pH2 and pH12 sample

REFERENCES

[1] J. Park, “Novel optofluidic sensor systems for quantitative chemical imaging and on-chip sensor calibration,” *Doctoral Dissertations*. 2009.

[2] S. Mine, “Meso-scale fluidic devices with chemical sensors for biological applications,” 2012.

[3] L. Rovati, P. Fabbri, and F. Pilati, “Development of a low-cost pH sensor based on plastic optical fibers,” in *2009 IEEE Intrumentation and Measurement Technology Conference*, 2009, pp. 1662–1665.

[4] F. Ferrero, I. Sanchez, J. Campo, J. M. Costa, J. Anton, M. Vega, and A. Sanz-Medel, “pH Measurements Using Simple Fiber-Optic Instrumentation and Luminescence Detection,” in *2005 IEEE Instrumentationand Measurement Technology Conference Proceedings*, 2005, vol. 2, pp. 1471–1475.

[5] S. Dutta, S. Basak, R. Kumar, and P. K. Samanta, “Fabrication of intensity based fiber optic pH sensor,” in *2010 3rd International Nanoelectronics Conference (INEC)*, 2010, pp. 370–371.

PAPER

I. OXYGEN DETERMINATION BASED ON OPTICAL MOUSE

ABSTRACT

In this research, an attempt is made to use easily accessible optoelectronic devices for sensing oxygen. An optical mouse is used as an oxygen sensor platform to explore the feasibility as an analytical device. An image sensor in the optical mouse is used for registering oxygen patch images with a band pass (615nm). The built-in red LED of the optical mouse was replaced with a blue LED (470nm peak) to excite the fluorescence responding to oxygen. Commercial RedEye™ oxygen-sensitive patches (fluorescence emission at 600 nm) based on the principle of fluorescence quenching was used as oxygen sensing element. A good sensitivity to oxygen was obtained with the optical mouse that may be useful to serve as optoanalytical devices for other chemical substances.

Keywords: oxygen, optoelectronic, optical mouse, fluorescence

1. INTRODUCTION

Optical oxygen sensors are particularly useful in the area of biological monitoring and chemical analysis because of their potential for remote detection and miniaturization. Optical oxygen sensors are becoming more common in many applications compared to traditional electrode oxygen. The optical oxygen sensor work on the principle that oxygen quenches the luminescence emitted from luminescent dyes that are immobilized in an oxygen permeable membrane [1].

In this research, an attempt is made to use easily accessible optoelectronic devices for sensing oxygen. An optical mouse is used as an oxygen sensor platform to explore the feasibility as an analytical device. Luminescence based optical oxygen measurement is achieved by registering images of a commercial oxygen sensor patch with an image sensor of optical mouse.

A blue light-emitting diode (470 nm peak) was used as light source to excite the luminophore responsive to oxygen [2]. A band pass filter (615 nm peak - FWHM 100 nm) was used to pass the fluorescence emission (600nm peak) from the oxygen patch. This approach enables the optical mouse to be used as a photodetector by capturing 2 dimensional 16x16 pixel gray scale images.

2. EXPERIMENTAL

2.1. Platform and Measurement Setup. A commercially available Logitech optical mouse (M/N: M-BJ69) was modified as an optical oxygen sensor platform by adding a gas channel beneath the optical mouse. Figure 1 is the diagram explaining the arrangement of optical mouse, bandpass filter (BPF) (5x5mm, 615 nm peak FWHM 100 nm from Optical Filter Shop/Pixelteq), LED, oxygen sensor patch. Red Eye oxygen sensor patch based on ruthenium complex from Ocean Optics was used as oxygen sensing element. To excite the fluorophore the default light source red LED inside the optical mouse has been replaced by blue LED (732-5019-1-ND) from Digi-Key Corporation with dominant wavelength of 465 nm. A 1.1 mm thick glass plate BPF at angle of incidence 0 degree was placed at the front of the image sensor lens to pass only the fluorescence emission and to increase oxygen sensitivity. The gap between the image sensor lens and oxygen patch is approximately 0.5 mm. The channel height and width is approximately 1 mm and 8 mm so that sufficient amount of gas is passed and there is enough room for oxygen patch for evaluation. The channel was formed using glass slides and adhesives. A commercial oxygen patch is placed beneath the image sensor. An opening of 8mm x 8mm square from the top surface of channel is exposed to image sensor for registering images. This exposed area can be reduced further depending on the oxygen sensor patch area and sensitivity. The top surface, bottom surface and edges of sensor platform is painted black to eliminate possible interference from ambient light.

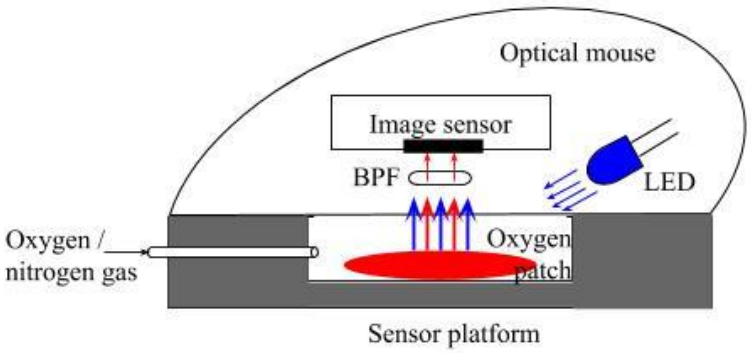

Figure 1. Cross-section of sensor platform based on optical mouse and commercial oxygen patch arrangement inside channel

Tube of 1 mm diameter is used to purge sample gas into the channel input. The open part of channel input was sealed with silicon adhesive and channel output was kept open intentional to drain out the gases. Dry oxygen and nitrogen gas cylinders from Airgas were used for experiment. MKS 247C 4 channel mass flow controller (MFC) was used to control the ratio of oxygen and nitrogen gases. MFC output connects to the sensor platform channel input via tube. The ratio of dry oxygen and nitrogen gases at 100 sccm were purged through the oxygen sensor platform. Different oxygen concentrations were obtained from 0-100% by mixing two streams of dry oxygen and nitrogen gas. Each stream was measured with a MFC and the mixture was passed over the oxygen sensor. Allowed gases to flow for 15 min for each ratio then registered six images of oxygen sensor for averaging the sensitivity. Using BPF significantly reduced “noise” colors of the other wavelength range that are not related with oxygen change. This experiment was performed in dark ambience to avoid any ambient light or external light interference.

2.2. Instrumentation. The following is the instrumentation setup for oxygen sensor analysis. To fetch the pixel data and transmitting them from mouse (optoelectronic device) via Arduino board to personal computer for evaluations [3]. The mouse is based on Optical Navigation Technology, contains an Image Acquisition System (IAS) and Digital Signal Processor (DSP). IAS acquires microscopic surface images via the lens under LED illumination. Figure 2 is the conceptual block diagram of overall experiment. First block consist of mouse and oxygen patch for analysis, second block consist of Arduino Duemilanove board, which plays a role of data mediator between mouse and third block. Arduino board is a single-board microcontroller built onto a single printed circuit board. It is used in this project as interface between mouse and PC. It is programmed to fetch the pixel data from mouse and transmit to PC. Third block is a personal computer that has java application running to receive and display the pixel data coming from mouse. This application also allows saving the live image [3].

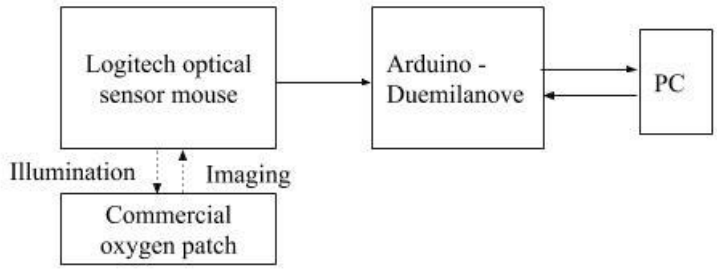

Figure 2. Conceptual block diagram of instrumentation

Commercially available Logitech optical mouse (M/N: M-BJ69) with ADNS 2051 image sensor inside mouse was used for image acquisition and integrated optical

structure for focusing the LED on oxygen patch. Five wires, each 0.5mm diameter 24-26 gauges is used to connect Arduino board and optical mouse. Figure 3 explains the detail pin connection between optical sensor and Arduino board. USB 2.0 Standard-B plug and receptacle is used for communication between Arduino board and PC. After the connection run java application on PC to display the live micro images [3].

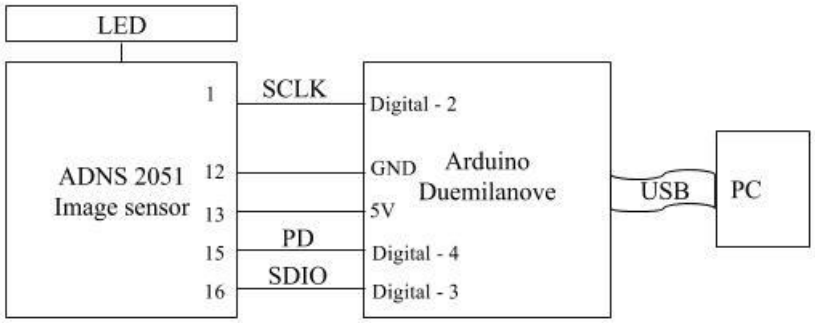

Figure 3. Pin configurations to connect image sensor and Arduino

2.3. Image Processing. Registered images from optical mouse are 16x16 pixels and pixel data ranges from zero for complete black, to 63 for complete white. The extraction of fluorescence emission intensity from the images is the important factor for calculating the oxygen concentration. The visible BPF enables to analyze the fluorescence emission intensity (red color) in gray scale and eliminate unnecessary and distorted information from the optical sensor. The total gray scale analysis is performed to translate the total mean of gray color intensity of the original images into oxygen concentration. The intensity measured is correlated to oxygen concentration using Stern-Volmer equation as follows:

$$I_o/I = 1 + Ksv\,[O_2] \quad (1)$$

$$Ksv = k\,I_o \quad (2)$$

Where I indicates luminescence intensity in the presence of oxygen (the subscript "o" denotes the absence of oxygen) and $[O_2]$, Ksv, k indicates oxygen concentration, Stern-Volmer constant and quencher rate coefficient, respectively. Emitted fluorescence light intensity from oxygen sensor changes in proportion to oxygen concentration, so by measuring emitted light intensity ratio (I_o/I) of fluorescence, oxygen concentration is determined.

The intensity of images registered when whole channel was saturated with nitrogen (i.e. 0% oxygen) represents Io of equation (1) and then intensities of different oxygen concentration represents I of equation (1). According to Stern-Volmer equation, Io/I need to be calculated for qualitative oxygen analysis and so the images registered at Io and I were divided with respect to each pixel number using Matlab [2]. A five-point calibration at 0%, 25%, 50%, 75% and 100% was carried out for quantitative oxygen analysis using optical mouse. Stern-Volmer equation helps in quantitative oxygen analysis.

MATLAB code was developed for analyzing the gray scale images taken at different oxygen concentrations and reconstructing the oxygen distribution images. In order to reduce the effect of noise image cropping and averaging techniques was employed by taking average of six images taken continuously at different oxygen concentrations [4].

3. RESULTS AND DISCUSSIONS

3.1. Micro Image Using Optical Mouse. Figure 4 displays 16x16 pixel registered images of commercial oxygen patch at 0% and 100 % of oxygen concentration. Intensity variation is in low scale but averaging the intensity of cropped image showed noticeable variation. Circled area is the region of interest which is cropped and used for evaluation as it contained the highest intensity variation. The total grayscale analysis was used to translate total mean of gray color intensity of the cropped images into oxygen concentration.

Figure 4. Gray scale original images of commercial oxygen patch taken with optical mouse with blue LED and bandpass filter at (a) 0% oxygen, (b) 100% oxygen

3.2. Oxygen Sensitivity. When oxygen molecules absorb light, electrons are excited and transit to single-term excitation state at higher energy than the stable base state. Part of the energy vibrates and rotates molecules for conversion to thermal energy, and settles in the single-term lowest excitation state. However, this excitation is exceedingly unstable, and electrons try to return to the original stable base state by releasing absorbed energy. Energy released by this transition emits light which is luminescence. In general when excitation light is irradiated the fluorophore immobilized on an oxygen patch, fluorescence is generated to form a charge transfer complex in the presence of oxygen molecules, and moves toward oxygen molecules, so fluorescence is extinguished by oxygen molecules quantitatively [5].

The oxygen-related emission from the oxygen patch has a peak wavelength 620 nm and spans in the range of 550-700 nm [6]. In the gray scale image analysis method, the patch image registered by the image sensor was taken into consideration to estimate the oxygen concentration. To achieve high sensitivity different regions of interest approximately around 10 x 10 pixels were analyzed and averaged within each and every image. From Figure 5 it can be stated that the average intensity of image decreased as oxygen concentration increases. Based on the Stern-Volmer equation, the Stern-Volmer plot shows a linear relationship between oxygen and Io/I.

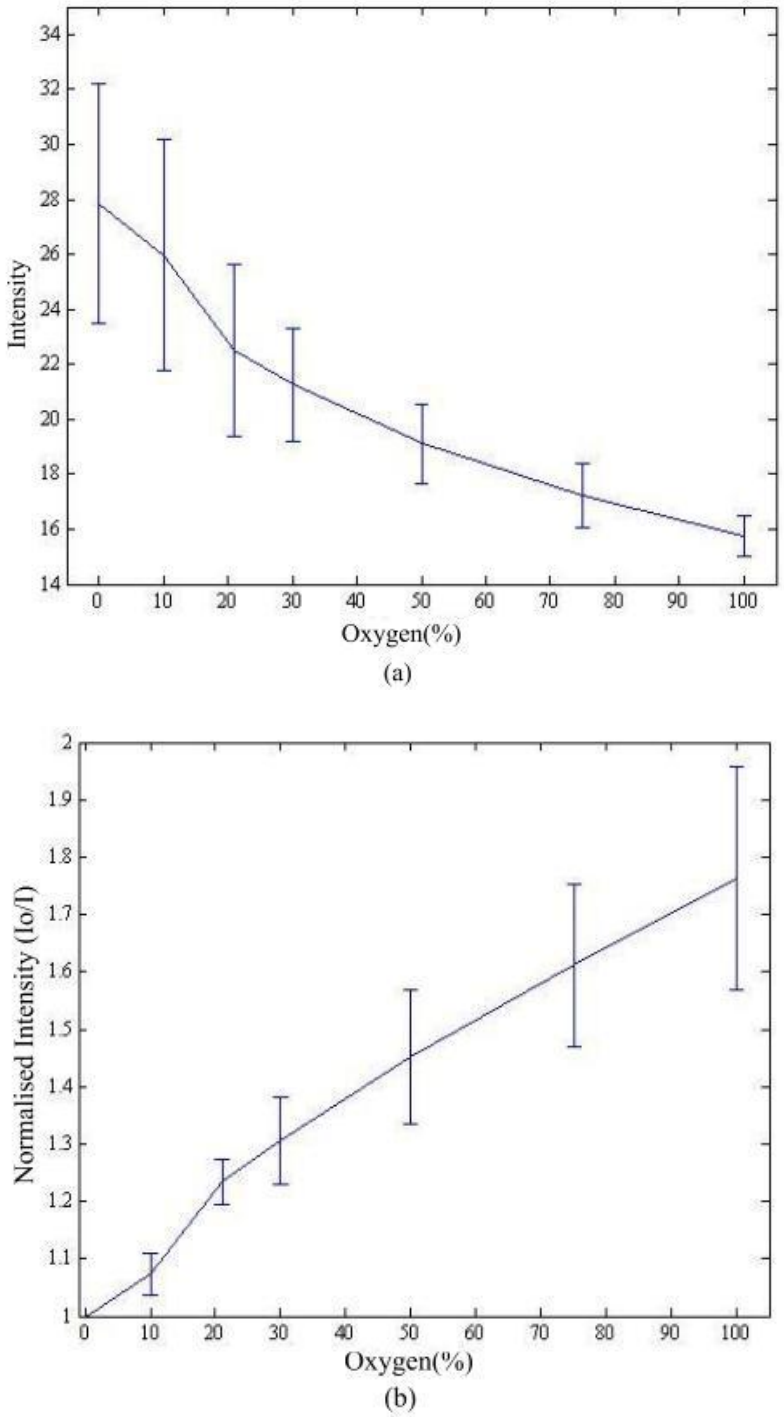

Figure 5. Oxygen sensitivity plot of three samples obtained with optical mouse (a) Intensity vs. oxygen concentration and (b) Stern-Volmer plot

4. CONCLUSION

The development of optical oxygen sensor platform based on low-cost easily accessible optoelectronic devices including optical mouse and LED has been successfully demonstrated. Preliminary results demonstrated that the ADNS 2051 image sensor of optical mouse has potential in capturing and sensing the required emission range. This confirms that optical mouse with blue LED can be used for detecting oxygen level. The proposed approach showed linearity and sensitivity and can be adapted to other optical biosensors using different luminophore. Moreover, the proposed technique is expected to serve as simple instrumentation setup for optical and functional imaging when analyzing biological samples.

REFERENCES

[1] J. Park, “Novel optofluidic sensor systems for quantitative chemical imaging and on-chip sensor calibration,” *Doctoral Dissertations*. 2009.

[2] S. Mine, “Meso-scale fluidic devices with chemical sensors for biological applications,” 2012.

[3] “Optical mouse camera - Bidouille.org.” [Online]. Available: http://www.bidouille.org/. [Accessed: 02-Apr-2015].

[4] J. Balsam, H. A. Bruck, Y. Kostov, and A. Rasooly, “Image stacking approach to increase sensitivity of fluorescence detection using a low cost complementary metal-oxide-semiconductor (CMOS) webcam.,” *Sens. Actuators. B. Chem.*, vol. 171–172, pp. 141–147, Jan. 2012.

[5] E. Toba, “Fiber optic fluorosensor for oxygen measurement,” in *IMTC/99. Proceedings of the 16th IEEE Instrumentation and Measurement Technology Conference (Cat. No.99CH36309)*, 1999, vol. 3, pp. 1426–1430.

[6] J. Park, C.-S. Kim, and Y. Kim, “A simple on-chip self-diagnosis/self-calibration method of oxygen microsensor using electrochemically generated bubbles,” *Sensors Actuators B Chem.*, vol. 108, no. 1–2, pp. 633–638, Jul. 2005.

II. PH ANALYSIS USING OPTICAL SENSOR

ABSTRACT

Optical sensor for chemical analysis is a growing technology since it offers many advantages. The goal of this research is to achieve pH sensing using low-cost optoelectronics devices such as optical mouse which consist of photodetector, light source and pre-installed optics. Colorimetric pH measurements were done with the optical mouse utilizing commercial pH test strips. All images were taken with an built-in image sensor of optical mice and the influence of factors for image acquisition such as optical filter, light source and gray scale image analysis method were evaluated. pH evaluation using spectrophotometer and digital camera were also conducted and compared with optical. The behavior of this sensing arrangement has been investigated for pH range between 2-12 providing reliable results.

Keywords: pH, optoelectronic, optical mouse, White LED, Colorimetric

1. INTRODUCTION

Monitoring of pH is required in many chemical reactions, biomedical diagnosis and environment surveillance. Basic principle of a classical pH strips was developed many decades ago [1]. Therefore simple low-cost optoelectronic devices of high stability and high detection sensitivity are in demand and expected to be developed.

An electronic imaging device used in optical mouse is a useful tool for quantitative chemical measurement [2]. Since the image sensor inside optical mouse can detect variation in optical intensities represented by pixels, it is possible to achieve instant two dimensional mapping of multiple colors in gray scale with the help of filters. Therefore we demonstrated novel idea of using optical mouse as colorimetric pH sensor.

Optical pH measurement method based on the color change from dyed cellulose matrix on the commercial Fisherbrand™ laboratory grade plastic pH strips was utilized. Seven pH buffer solutions by FisherScientific™ were selected for wide pH measurement. The pH valuation is based on measuring the reflected light intensity and rate of absorption when there is a change in color of pH indicator covalently immobilized on the cellulose matrix [3]. Thus the pH value of the solution is obtained from the analysis of the registered grayscale images. To verify the proposed grayscale image analysis method, results were compared with those of spectrometric measurements, RGB analysis result and color absorption theory [4].

2. COLOR THEORY

Optical effects contribute to convert the pH of the solution into the spectral information [1]. Absorption is the phenomena governing the photons propagating through the optical sensor and determining the intensity and spectral properties of the reflected

light. Absorption of light by a pH test strip occurs because the selected frequency of the illuminated light matches the frequency at which electrons in the atoms of the pH strip material vibrate. If any light that does not have enough or has excessive energy cannot be absorbed is reflected [5].

Figure 1 demonstrates the light absorption and reflection as per pH strip color. The information of interest is strictly associated to selective absorption of light by the pH test strip. The color results of the pH strip are in range starts from red (pH2) goes to yellow (pH6), green (pH8) and blue (pH12). A change in color induces a change in the intensities of the reflected light collected by the image sensor. In pH2 the result color is red so it reflects the most of incident red light. This is due to the fact that the red color component absorbs all color light but red light [6]. Whereas pH12 falls in blue color family which absorbs most of red light. Thus pH value of the solution can be obtained from the analysis of the reflected light emission intensities and red light absorption.

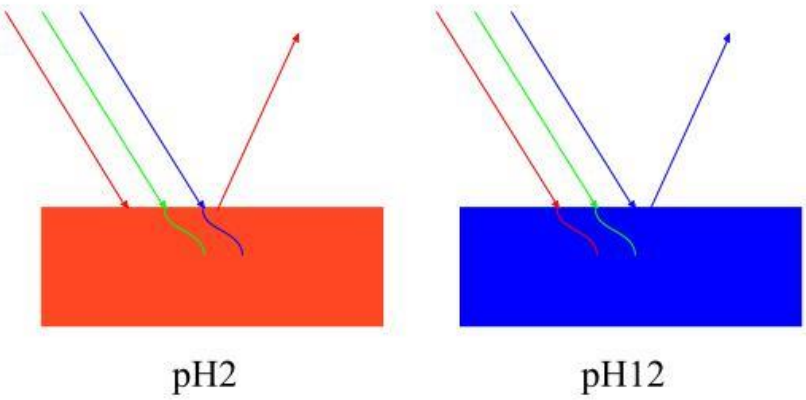

Figure 1. Color absorption and reflection of pH test strips in pH2 (red) and pH12 (blue) sample

3. EXPERIMENTAL

3.1. Platform and Measurement Setup. A commercially available Logitech optical mouse (M/N: M-BJ69) was modified as an optical pH sensor platform by adding a channel beneath the optical mouse to hold test sample. Figure 2 is the diagram explaining the arrangement of optical mouse, bandpass filter (BPF) (5x5mm, 615 nm peak FWHM 100 nm from Optical Filter Shop/Pixelteq), LED and pH test strip.

Fisherbrand™ laboratory grade plastic pH strips were used for examination. These pH strips consists of a 0.5 in. (1.27cm) cellulose matrix contain dye which changes color according to pH buffer solution. Seven pH buffer solutions by FisherScientific™ were selected for wide pH measurement range. The expected color changes with respect to buffer solutions are red-orange for pH2, orange for pH4, yellow for pH6, yellow-green for pH7, green for pH8, green-blue for pH10 and dark blue for pH 12. The BPF is used to filter the reflected light from pH strip.

A 1.1 mm thick glass plate BPF at angle of incidence 0 degree was placed at the front of the image sensor lens to pass only the fluorescence emission and to increase pH sensitivity. The open channel is made in center of the platform to slide the pH strip for evaluation. The length of channel is calculated such that the pH sensitive cellulose matrix stops in front of optical sensor lens and channel width is 1 mm more than the width of pH strip. The top surface, bottom surface and edges of sensor platform are painted black to eliminate possible interference from ambient light.

Placed mouse on the pH sensor platform such that optical sensor lens is facing pH strip. The gap between optical sensor lens and pH sensitive area was kept approximately 3 mm. A 0.016 ml of pH buffer solution is dropped on a pH strip and images were taken

after 30 seconds so that the pH strip absorbs the buffer solution and changes its color completely. Using optical mouse the images of each pH strip was registered in grayscale.

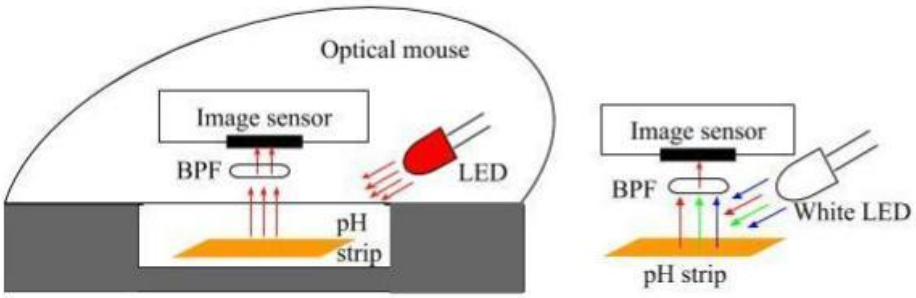

Figure 2. Cross-section of sensor platform based on optical mouse and commercial pH strip arrangement inside channel

Two different series of experiments were performed for pH strip imaging and valuation: (1) Red light source with BPF and (2) white light source with or without BPF. The purpose of the two series of experiments was to compare the effectiveness of the red and white LED in quantitative pH valuation.

3.2. Instrumentation. The following is the instrumentation setup for pH sensor analysis. To fetch the pixel data and transmitting them from mouse (optoelectronic device) via Arduino board to personal computer for evaluations [7]. The mouse is based on Optical Navigation Technology, contains an Image Acquisition System (IAS) and Digital Signal Processor (DSP). IAS acquires microscopic surface images via the lens under LED illumination. Figure 3 is the conceptual block diagram of overall experiment. First block consist of mouse and pH test strip for analysis, second block consist of Arduino Duemilanove board, which plays a role of data mediator between mouse and

third block. Arduino board is a single-board microcontroller built onto a single printed circuit board. It is used in this project as interface between mouse and PC. It is programmed to fetch the pixel data from mouse and transmit to PC. Third block is a personal computer that has java application running to receive and display the pixel data coming from mouse. This application also allows to save the live image [7].

.

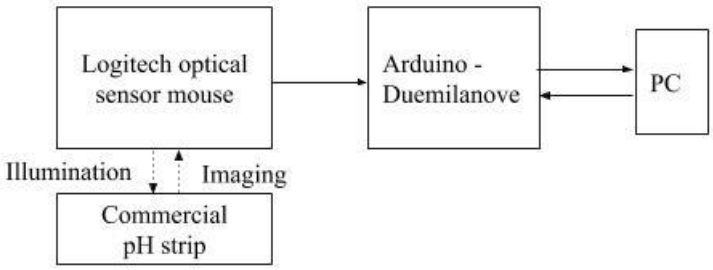

Figure 3. Conceptual block diagram of instrumentation

Commercially available Logitech optical mouse (M/N: M-BJ69) with ADNS 2051 image sensor inside mouse was used for image acquisition and integrated optical structure for focusing the LED on pH test strip. Five wires, each 0.5mm diameter 24-26 gauges is used to connect Arduino board and optical mouse. Figure 4 explains the detail pin connection between optical sensor and Arduino board. USB 2.0 Standard-B plug and receptacle is used for communication between Arduino board and PC. After the connection run java application on PC to display the live micro images [7].

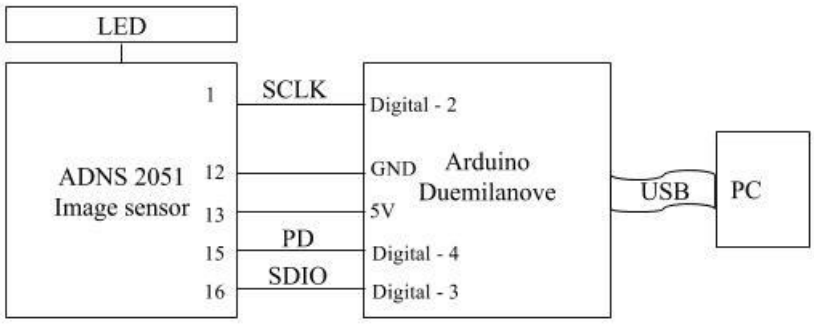

Figure 4. Pin configurations to connect image sensor and Arduino

4. IMAGE PROCESSING

In general, pH test strip is based on pH-induced reversible changes in the optical properties (i.e. absorbance and reflectance) of an immobilized pH indicator [8]. In our case the information of interest is strictly associated to selective absorption of red light operated by the pH sensitive cellulose matrix on pH strip. So extraction of red light from the reflected light by pH strip is the main factor for pH valuation. The visible BPF enables to analyze this factor in grayscale and eliminate unnecessary and distorted information from the pH strip.

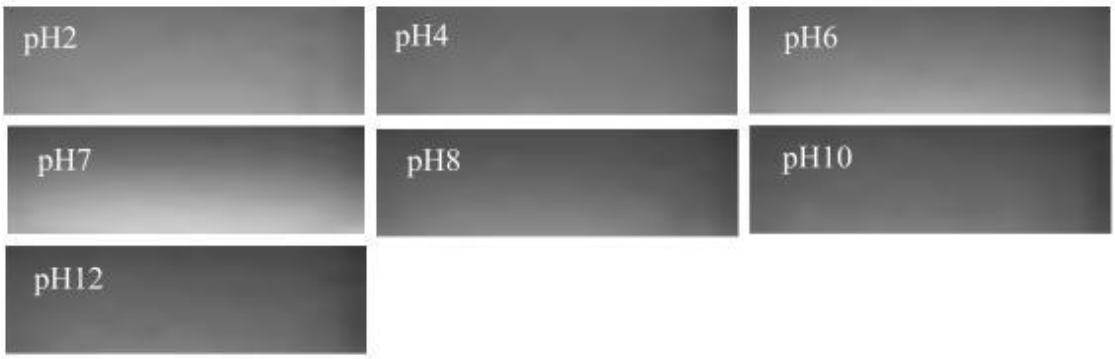

Figure 5. Grayscale cropped images of a commercial pH test strip taken with optical mouse with BPF under red LED illumination

Figure 5 displays registered images where pixel data ranges from zero for complete black, to 63 for complete white. The total grayscale analysis was used to translate total mean of gray color intensity of the original images into pH valuation. MATLAB codes were developed for processing grayscale images [9]. The process consist of three steps after image acquisitions, which are respectively: reading image, cropping the region of interest and averaging pixel value of each cropped image [10]. The average pixel value measured is correlated to red intensity in the reflected light. These intensities from pH strips were plotted with error bars using Matlab script which indicate the standard deviation of mean of seven independent measurements.

5. RESULTS AND DISCUSSION

5.1. White Light Source With and Without BPF. The spectral output of the white LED source is plotted in Figure 6 (a) ranging from 420 nm to 700 nm. The required red component has highest intensity than others. The green and blue component results into noise and is removed using BPF, whereas the red component is capable enough to obtain intensity linear curve.

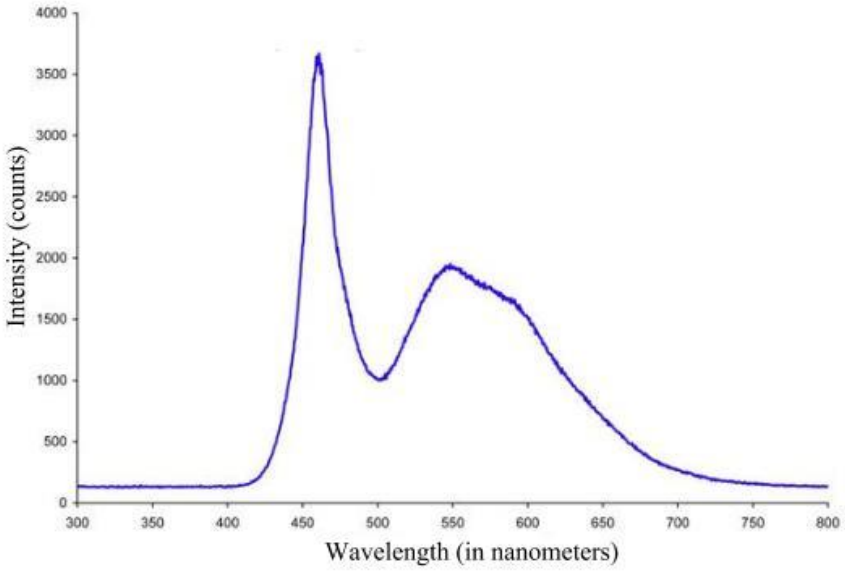

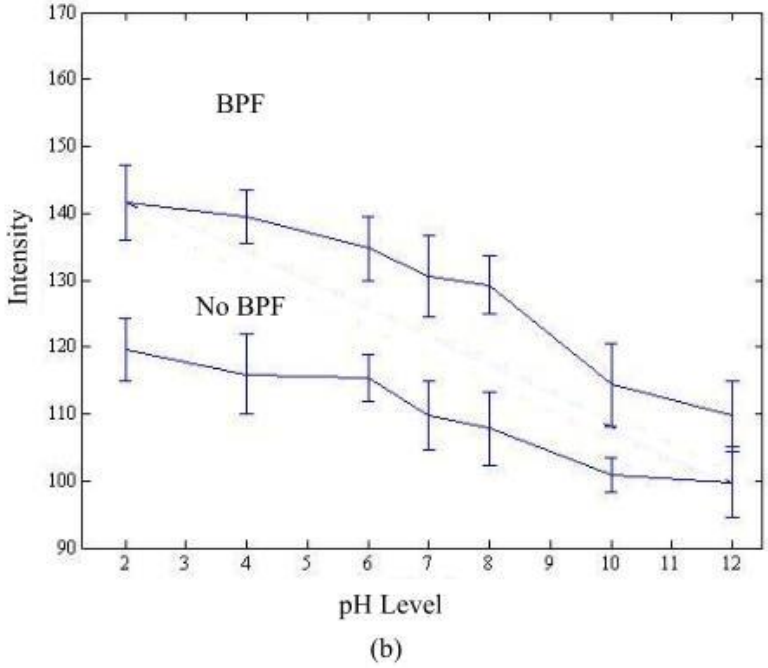

Figure 6. (a) Spectral output of the white LED. Reprinted from Digi-Key, by Steven Keeping, 2011, http://www.digikey.com (b) pH sensitivity obtained with optical mouse under white LED illumination

Taking into consideration that ADNS 2051 image sensor is more sensitive to red wavelength and to test the effect of BPF on the measurement, pH strip images were registered without BPF. Figure 6(b) shows the characteristic of reflected intensities from the pH strips and the standard deviation without the filter. The sensitivity degradation to a certain extent is expected without BPF because of the interfering wavelength other than red. Although the white light source without filtering shows the least linearity than the other, it still exhibits a reasonable sensitivity between extreme pH levels without much degradation in the standard deviation. This approach can be used to detect extreme pH level like pH2 and pH12.

5.2. Red Light Source With BPF. To check the pH valuation efficiency with red light and BPF, white LED was replaced by red. The red LED used is the default optical mouse LED with 639 nm peak. Figure 7 shows the linear characteristics of reflected intensities from the pH strips and the standard deviation of mean of seven samples for each pH level. It should be noted that the intensity curve has higher sensitivity than the previous experiment and is quantitative to differentiate the pH level. This is because the main source of light is red LED and visible BPF helped in removing information not related with the pH measurement. Therefore regardless of the kind of light source, the grayscale analysis of red light intensities showed perceptible linearity.

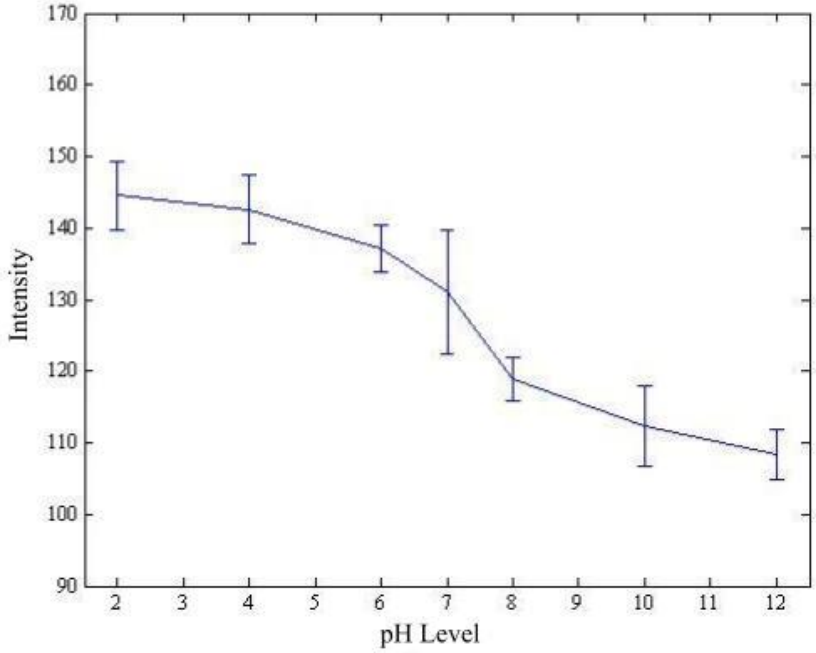

Figure 7 pH sensitivity obtained with optical mouse with bandpass filter under red LED illumination

5.3. pH Color Analysis Using Spectrometer. In parallel with characterizing the pH strip using optical mouse, it has to be confirmed that the red component in the reflected light from the pH strip is gradually decreasing with increase in pH level. Three samples for each pH level were analyzed using the spectrophotometer (USB4000, Ocean Optics) to confirm the variation due to absorption of red light. A reflection probe (R400-7-UV-VIS, Ocean Optics), consisting of one read fiber (400 μm diameter) was used to capture reflectance from the pH strip. The reflection probe was placed such that reflected light was detected without direct interference of the light source. The spectra of the three pH samples are represented in figure 8 with red LED illumination.

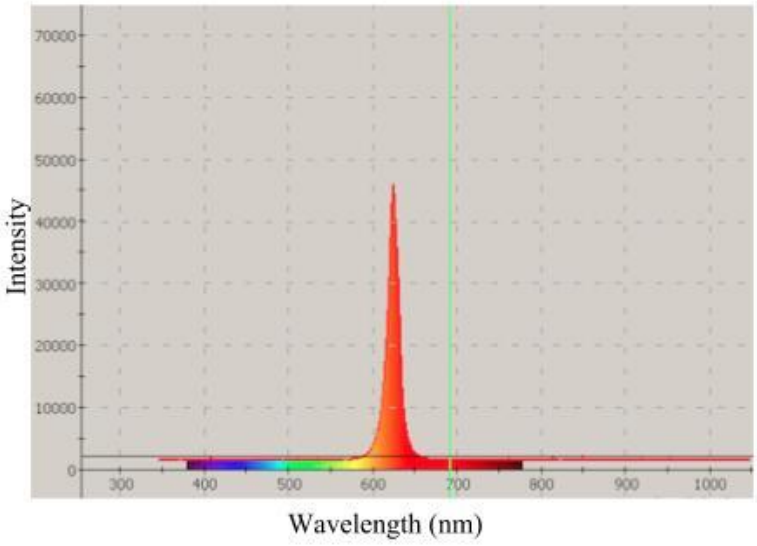

(a)

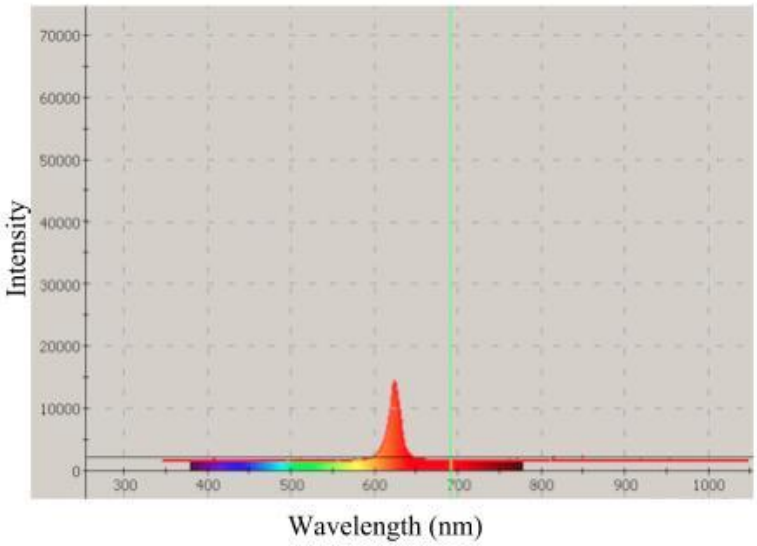

(b)

Figure 8. Spectra of reflected light from pH test strip under red LED illumination (a) pH2 (b) pH7 (c) pH12

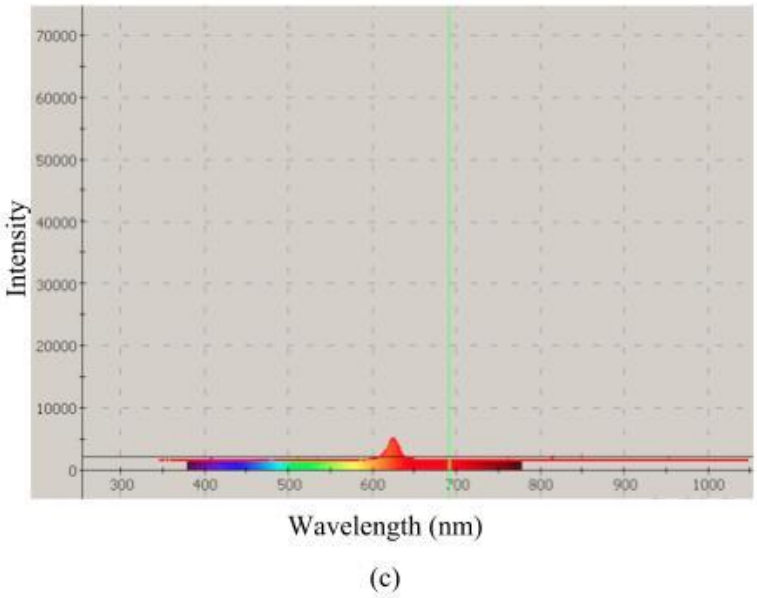

Figure 8. Spectra of reflected light from pH test strip under red LED illumination (a) pH2 (b) pH7 (c) pH12 (cont.)

To avoid any sort of error the data were recorded for three samples for each pH level. The measured spectral range covers the visible spectrum from 300 to 800 nm. From the Figure 9, we can state that the red peak intensity decreases as pH level increases in both the cases. It shows that the changes in reflected light are easily detected in terms of peak intensity and corresponding wavelength. Similar linearity was seen in the intensity level while analyzing the pH strip under optical mouse. This confirms that the optical mouse with red or white LED can be used as intensity dependent method for pH valuation.

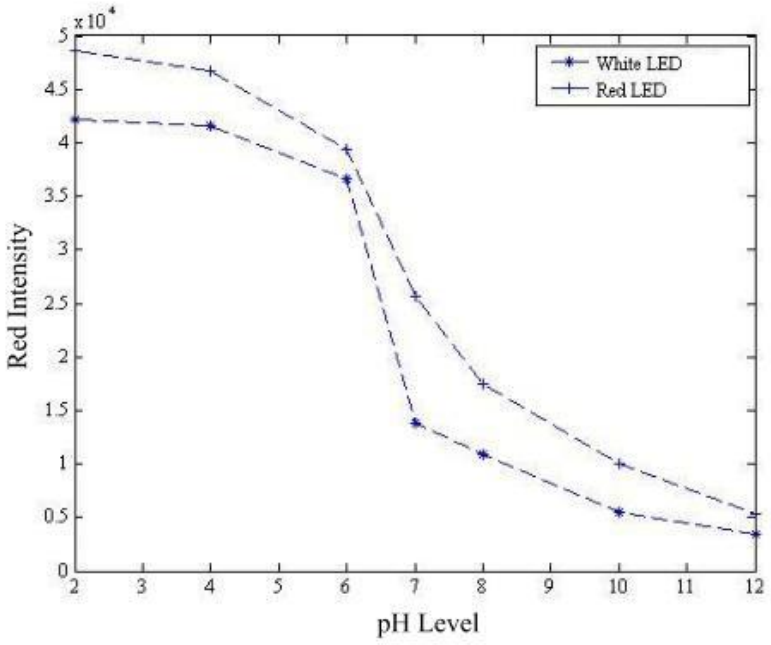

Figure 9. Decrease of red intensity peak (630 nm) reflected from pH test strips obtained with spectrometer

5.4. RGB Analysis Of pH Colors. A color CCD camera (DS-5M, Bayer-masked, Nikon) was used for color image acquisition of pH strip for evaluating the red, green and blue intensities. The pH strips color images were registered under white light. Figure 10 (a) displays the original color images of pH strips. The cropped color images were analyzed in RGB color space in the MATLAB script to study the behavior of individual reflected light intensities. The total RGB intensities from each image corresponding to each pH strip is plotted in Figure 10 (b). From figure it can be stated that the red intensity decreases with increase in pH level. A similar trend of red intensity was observed as compared to spectrometric and optical mouse data.

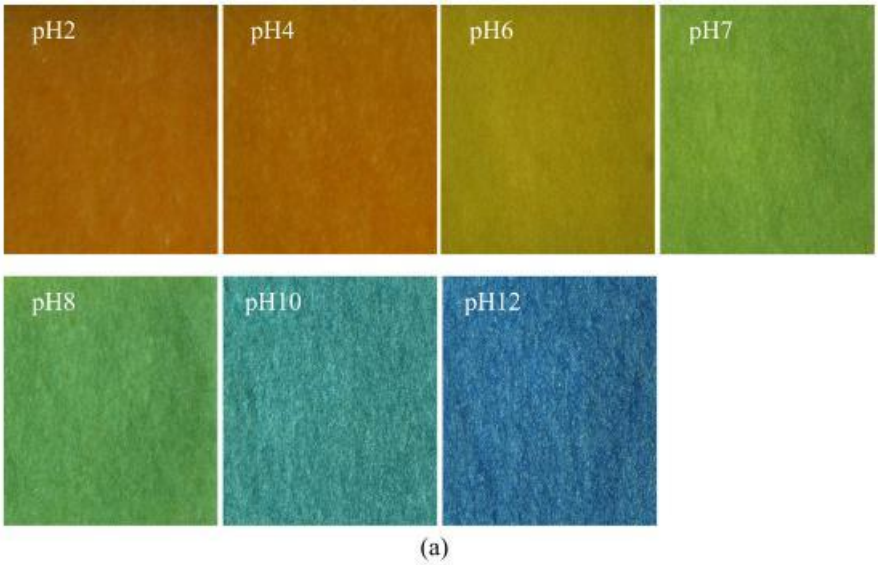

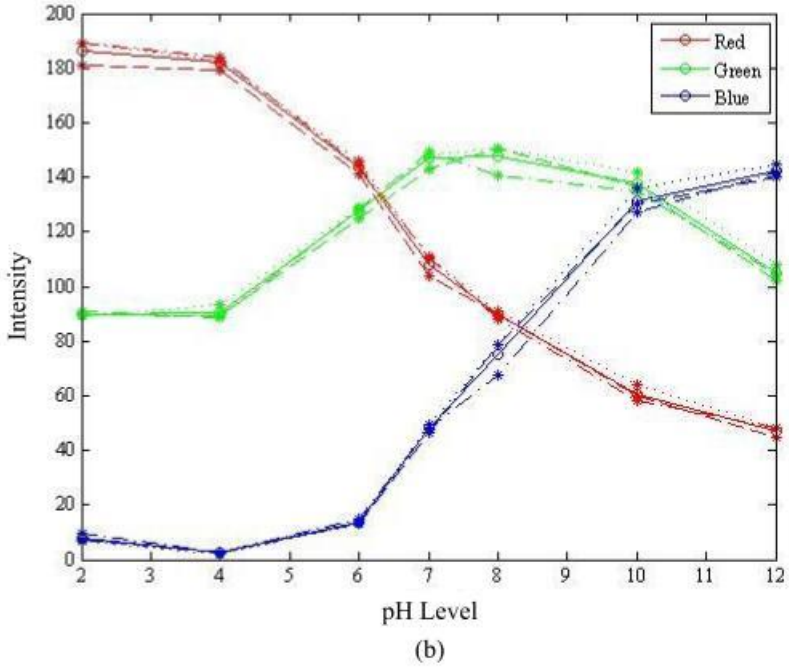

Figure 10 RGB analysis (a) Cropped color images of pH test strips obtained with color camera (b) RGB intensities of each pH level

6. CONCLUSION AND FUTURE WORK

The development of a pH optical sensor platform, based on a low-cost optical mouse has been presented. Preliminary results demonstrated that the image sensor in the optical mouse exhibits a good sensitivity for differentiating pH level under red LED or white LED. The optical pH sensor platform can therefore be implemented using any low cost optoelectronics devices which is capable of capturing images and transmitting pixel data. This approach offers an affordable and reliable solution for checking pH level of samples.

Future plan includes adopting color sensor, improving the registered image spatial resolution and increasing the pH detection range whereas a complete characterization of the overall setup in terms of sensitivity and linearity.

REFERENCES

[1] L. Rovati, P. Fabbri, and F. Pilati, "Development of a low-cost pH sensor based on plastic optical fibers," in *2009 IEEE Intrumentation and Measurement Technology Conference*, 2009, pp. 1662–1665.

[2] L. Shen, J. A. Hagen, and I. Papautsky, "Point-of-care colorimetric detection with a smartphone.," *Lab Chip*, vol. 12, no. 21, pp. 4240–3, Nov. 2012.

[3] R. Wolthuis, D. McCrae, E. Saaski, J. Hartl, and G. Mitchell, "Development of a medical fiber-optic pH sensor based on optical absorption.," *IEEE Trans. Biomed. Eng.*, vol. 39, no. 5, pp. 531–7, May 1992.

[4] R. Prien, "Technologies for new in situ chemical sensors," in *OCEANS 2007 - Europe*, 2007, pp. 1–6.

[5] F. Ferrero, I. Sanchez, J. Campo, J. M. Costa, J. Anton, M. Vega, and A. Sanz-Medel, "pH Measurements Using Simple Fiber-Optic Instrumentation and Luminescence Detection," in *2005 IEEE Instrumentationand Measurement Technology Conference Proceedings*, 2005, vol. 2, pp. 1471–1475.

[6] S. Dutta, S. Basak, R. Kumar, and P. K. Samanta, "Fabrication of intensity based fiber optic pH sensor," in *2010 3rd International Nanoelectronics Conference (INEC)*, 2010, pp. 370–371.

[7] "Optical mouse camera - Bidouille.org." [Online]. Available: http://www.bidouille.org/. [Accessed: 02-Apr-2015].

[8] F. J. FerreroMartin, J. C. CampoRodriguez, J. C. AlvarezAnton, J. C. VieraPerez, I. Sanchez-Barragan, J. M. Costa-Fernandez, and A. Sanz-Medel, "Design of a Low-Cost Optical Instrument for pH Fluorescence Measurements," *IEEE Trans. Instrum. Meas.*, vol. 55, no. 4, pp. 1215–1221, Aug. 2006.

[9] S. Mine, "Meso-scale fluidic devices with chemical sensors for biological applications," 2012.

[10] J. Balsam, H. A. Bruck, Y. Kostov, and A. Rasooly, "Image stacking approach to increase sensitivity of fluorescence detection using a low cost complementary metal-oxide-semiconductor (CMOS) webcam.," *Sens. Actuators. B. Chem.*, vol. 171–172, pp. 141–147, Jan. 2012.

SECTION

2. CONCLUSION

Image sensor inside optical mouse exhibits a good linearity and sensitivity for detecting oxygen concentration and differentiating pH level under LED illumination with BPF. Optical sensor platform can therefore be implemented using any low cost optoelectronic devices which are capable of capturing images and processing them. Hence the proposed approach can be adapted to other optical biosensors using different luminophores (fluorophores, phosphores, etc.).

Future work includes adopting image sensor capable of registering image at high bit-depth per pixel for improving the image resolution and increasing the sensitivity and standardizing sensor platform design for consistent measurements in terms of sensitivity and linearity.

APPENDIX A

MATLAB CODE (M-FILE) FOR IMAGE PROCESSING OF PAPER I

The MATLAB m- file to produce figure 5 in paper I as follows:

```
clc; clear; close all;
% Read the cropped grayscale images and store them in double array
crop_area = [1.5 1.5 14 12];
% 0% Oxygen
im_01_esy=double(imcrop((imread('exp30_0_perc_5.png')),crop_area));
im_02_esy=double(imcrop((imread('exp30_0_perc_6.png')),crop_area));
im_03_esy=double(imcrop((imread('exp30_0_perc_7.png')),crop_area));
im_04_esy=double(imcrop((imread('exp30_0_perc_8.png')),crop_area));
im_05_esy=double(imcrop((imread('exp30_0_perc_9.png')),crop_area));
im_06_esy=double(imcrop((imread('exp30_0_perc_10.png')),crop_area));
%25% Oxygen
im_251_esy=double(imcrop((imread('exp30_25_perc_5.png')),crop_area));
im_252_esy=double(imcrop((imread('exp30_25_perc_6.png')),crop_area));
im_253_esy=double(imcrop((imread('exp30_25_perc_7.png')),crop_area));
im_254_esy=double(imcrop((imread('exp30_25_perc_8.png')),crop_area));
im_255_esy=double(imcrop((imread('exp30_25_perc_9.png')),crop_area));
im_256_esy=double(imcrop((imread('exp30_25_perc_10.png')),crop_area));
%50% Oxygen
im_501_esy=double(imcrop((imread('exp30_50_perc_5.png')),crop_area));
im_502_esy=double(imcrop((imread('exp30_50_perc_6.png')),crop_area));
im_503_esy=double(imcrop((imread('exp30_50_perc_7.png')),crop_area));
```

```
im_504_esy=double(imcrop((imread('exp30_50_perc_8.png')),crop_area));
im_505_esy=double(imcrop((imread('exp30_50_perc_9.png')),crop_area));
im_506_esy=double(imcrop((imread('exp30_50_perc_10.png')),crop_area));
%75% Oxygen
im_751_esy=double(imcrop((imread('exp30_75_perc_5.png')),crop_area));
im_752_esy=double(imcrop((imread('exp30_75_perc_6.png')),crop_area));
im_753_esy=double(imcrop((imread('exp30_75_perc_7.png')),crop_area));
im_754_esy=double(imcrop((imread('exp30_75_perc_8.png')),crop_area));
im_755_esy=double(imcrop((imread('exp30_75_perc_9.png')),crop_area));
im_756_esy=double(imcrop((imread('exp30_75_perc_10.png')),crop_area));
% 100% Oxygen
im_1001_esy=double(imcrop((imread('exp30_100_perc_5.png')),crop_area));
im_1002_esy=double(imcrop((imread('exp30_100_perc_6.png')),crop_area));
im_1003_esy=double(imcrop((imread('exp30_100_perc_7.png')),crop_area));
im_1004_esy=double(imcrop((imread('exp30_100_perc_8.png')),crop_area));
im_1005_esy=double(imcrop((imread('exp30_100_perc_9.png')),crop_area));
im_1006_esy=double(imcrop((imread('exp30_100_perc_10.png')),crop_area));
% Averaging intensity of 0% Oxygen
mean_01 = mean2(im_01_esy);
mean_02 = mean2(im_02_esy);
mean_03 = mean2(im_03_esy);
mean_04 = mean2(im_04_esy);
mean_05 = mean2(im_05_esy);
```

```
mean_06 = mean2(im_06_esy);
mean_0_array=[mean_01;mean_02;mean_03;mean_04;mean_05; mean_06];
mean_0=mean(mean_0_array);
% Averaging intensity of 25% Oxygen
mean_251 = mean2(im_251_esy);
mean_252 = mean2(im_252_esy);
mean_253 = mean2(im_253_esy);
mean_254 = mean2(im_254_esy);
mean_255 = mean2(im_255_esy);
mean_256 = mean2(im_256_esy);
mean_25_array=[mean_251;mean_252;mean_253;mean_254;mean_255;mean_256];
mean_25=mean(mean_25_array);
% Averaging intensity of 50% Oxygen
mean_501 = mean2(im_501_esy);
mean_502 = mean2(im_502_esy);
mean_503 = mean2(im_503_esy);
mean_504 = mean2(im_504_esy);
mean_505 = mean2(im_505_esy);
mean_506 = mean2(im_506_esy);
mean_50_array=[mean_501;mean_502;mean_503;mean_504;mean_505;mean_506];
mean_50=mean(mean_50_array);
% Averaging intensity of 75% Oxygen
mean_751 = mean2(im_751_esy);
```

```
mean_752 = mean2(im_752_esy);

mean_753 = mean2(im_753_esy);

mean_754 = mean2(im_754_esy);

mean_755 = mean2(im_755_esy);

mean_756 = mean2(im_756_esy);

mean_75_array=[mean_751;mean_752;mean_753;mean_754;mean_755;mean_756];

mean_75=mean(mean_75_array);

% Averaging intensity of 100% Oxygen

mean_1001 = mean2(im_1001_esy);

mean_1002 = mean2(im_1002_esy);

mean_1003 = mean2(im_1003_esy);

mean_1004 = mean2(im_1004_esy);

mean_1005 = mean2(im_1005_esy);

mean_1006 = mean2(im_1006_esy);

mean_100_array=[mean_1001;mean_1002;mean_1003;mean_1004;mean_1005;

mean_1006];

mean_100=mean(mean_100_array);

%Array of average pixel value of all concentrations (Y-axis)

%Array of Saturated oxygen percentage (X-axis)

avg_pixel_array=[mean_0, mean_25, mean_50, mean_75, mean_100];

oxy_value=[ 0, 25, 50, 75,100];

% plot result

figure();
```

```
avg_pixel_plot=plot(oxy_value, avg_pixel_array,'b--*');
title('Oxy Perc - Normalised Intensity (BPF(605nm) / Blue Led)');
xlabel('Oxygen(%sat.)');
ylabel('Avg Pixel');
%Calculating as per Stern-Volmer equation
SV_0=mean_0/mean_0;
SV_25=mean_0/mean_25;
SV_50=mean_0/mean_50;
SV_75=mean_0/mean_75;
SV_100=mean_0/mean_100;
%Array of Io/I of all concentrations (Y-axis)
%Array of Saturated oxygen percentage (X-axis)
SV=[SV_0,SV_25, SV_50, SV_75, SV_100];
X = [0, 25, 50, 75, 100];
figure();
pH_plot=plot(X, SV,'b--*');
title('Stern-Volmer');
xlabel( 'Oxygen(%sat.)' );
ylabel('Normalized Intensity (Io/I)'
.
```

APPENDIX B

MATLAB CODE (M-FILE) FOR IMAGE PROCESSING OF PAPER II

The MATLAB m- file to produce figure 7 in paper II as follows:

```
clc; clear; close all;
%Reading cropped images of seven different pH strip sample for each pH
%buffer solution
crop_area = [0.5 0.5 16 06];
% pH2
im_2_esy_s1_1=double(imcrop((imread('Exp26_pH2_S1.png')),crop_area));
im_2_esy_s2_1=double(imcrop((imread('Exp26_pH2_S2.png')),crop_area));
im_2_esy_s3_1=double(imcrop((imread('Exp26_pH2_S3.png')),crop_area));
im_2_esy_s4_1=double(imcrop((imread('Exp26_pH2_S4.png')),crop_area));
im_2_esy_s5_1=double(imcrop((imread('Exp26_pH2_S5.png')),crop_area));
im_2_esy_s6_1=double(imcrop((imread('Exp26_pH2_S6.png')),crop_area));
im_2_esy_s7_1=double(imcrop((imread('Exp26_pH2_S7.png')),crop_area));
% pH4
im_4_esy_s1_1=double(imcrop((imread('Exp26_pH4_S1.png')),crop_area));
im_4_esy_s2_1=double(imcrop((imread('Exp26_pH4_S2.png')),crop_area));
im_4_esy_s3_1=double(imcrop((imread('Exp26_pH4_S3.png')),crop_area));
im_4_esy_s4_1=double(imcrop((imread('Exp26_pH4_S4.png')),crop_area));
im_4_esy_s5_1=double(imcrop((imread('Exp26_pH4_S5.png')),crop_area));
im_4_esy_s6_1=double(imcrop((imread('Exp26_pH4_S6.png')),crop_area));
im_4_esy_s7_1=double(imcrop((imread('Exp26_pH4_S7.png')),crop_area));
% pH6
```

```
im_6_esy_s1_1=double(imcrop((imread('Exp26_pH6_S1.png')),crop_area));
im_6_esy_s2_1=double(imcrop((imread('Exp26_pH6_S2.png')),crop_area));
im_6_esy_s3_1=double(imcrop((imread('Exp26_pH6_S3.png')),crop_area));
im_6_esy_s4_1=double(imcrop((imread('Exp26_pH6_S4.png')),crop_area));
im_6_esy_s5_1=double(imcrop((imread('Exp26_pH6_S5.png')),crop_area));
im_6_esy_s6_1=double(imcrop((imread('Exp26_pH6_S6.png')),crop_area));
im_6_esy_s7_1=double(imcrop((imread('Exp26_pH6_S7.png')),crop_area));
%pH7
im_7_esy_s1_1=double(imcrop((imread('Exp26_pH7_S1.png')),crop_area));
im_7_esy_s2_1=double(imcrop((imread('Exp26_pH7_S2.png')),crop_area));
im_7_esy_s3_1=double(imcrop((imread('Exp26_pH7_S3.png')),crop_area));
im_7_esy_s4_1=double(imcrop((imread('Exp26_pH7_S4.png')),crop_area));
im_7_esy_s5_1=double(imcrop((imread('Exp26_pH7_S5.png')),crop_area));
im_7_esy_s6_1=double(imcrop((imread('Exp26_pH7_S6.png')),crop_area));
im_7_esy_s7_1=double(imcrop((imread('Exp26_pH7_S7.png')),crop_area));
%pH8
im_8_esy_s1_1=double(imcrop((imread('Exp26_pH8_S1.png')),crop_area));
im_8_esy_s2_1=double(imcrop((imread('Exp26_pH8_S2.png')),crop_area));
im_8_esy_s3_1=double(imcrop((imread('Exp26_pH8_S3.png')),crop_area));
im_8_esy_s4_1=double(imcrop((imread('Exp26_pH8_S4.png')),crop_area));
im_8_esy_s5_1=double(imcrop((imread('Exp26_pH8_S5.png')),crop_area));
im_8_esy_s6_1=double(imcrop((imread('Exp26_pH8_S6.png')),crop_area));
im_8_esy_s7_1=double(imcrop((imread('Exp26_pH8_S7.png')),crop_area));
```

```
% pH10
im_10_esy_s1_1=double(imcrop((imread('Exp26_pH10_S1.png')),crop_area));
im_10_esy_s2_1=double(imcrop((imread('Exp26_pH10_S2.png')),crop_area));
im_10_esy_s3_1=double(imcrop((imread('Exp26_pH10_S3.png')),crop_area));
im_10_esy_s4_1=double(imcrop((imread('Exp26_pH10_S4.png')),crop_area));
im_10_esy_s5_1=double(imcrop((imread('Exp26_pH10_S5.png')),crop_area));
im_10_esy_s6_1=double(imcrop((imread('Exp26_pH10_S6.png')),crop_area));
im_10_esy_s7_1=double(imcrop((imread('Exp26_pH10_S7.png')),crop_area));
% pH12
im_12_esy_s1_1=double(imcrop((imread('Exp26_pH12_S1.png')),crop_area));
im_12_esy_s2_1=double(imcrop((imread('Exp26_pH12_S2.png')),crop_area));
im_12_esy_s3_1=double(imcrop((imread('Exp26_pH12_S3.png')),crop_area));
im_12_esy_s4_1=double(imcrop((imread('Exp26_pH12_S4.png')),crop_area));
im_12_esy_s5_1=double(imcrop((imread('Exp26_pH12_S5.png')),crop_area));
im_12_esy_s6_1=double(imcrop((imread('Exp26_pH12_S6.png')),crop_area));
im_12_esy_s7_1=double(imcrop((imread('Exp26_pH12_S7.png')),crop_area));
% Averaging
mean_2_S1 = mean2(im_2_esy_s1_1);
mean_2_S2 = mean2(im_2_esy_s2_1);
mean_2_S3 = mean2(im_2_esy_s3_1);
mean_2_S4 = mean2(im_2_esy_s4_1);
mean_2_S5 = mean2(im_2_esy_s5_1);
mean_2_S6 = mean2(im_2_esy_s6_1);
```

```
mean_2_S7 = mean2(im_2_esy_s7_1);
mean_2_best = max ([mean_2_S1,mean_2_S2, mean_2_S3,mean_2_S4, mean_2_S5,
mean_2_S6, mean_2_S7]);
mean_4_S1 = mean2(im_4_esy_s1_1);
mean_4_S2 = mean2(im_4_esy_s2_1);
mean_4_S3 = mean2(im_4_esy_s3_1);
mean_4_S4 = mean2(im_4_esy_s4_1);
mean_4_S5 = mean2(im_4_esy_s5_1);
mean_4_S6 = mean2(im_4_esy_s6_1);
mean_4_S7 = mean2(im_4_esy_s7_1);
mean_4_best = mean ([mean_4_S1,mean_4_S2, mean_4_S3,mean_4_S4, mean_4_S5,
mean_4_S6, mean_4_S7]);
mean_6_S1 = mean2(im_6_esy_s1_1);
mean_6_S2 = mean2(im_6_esy_s2_1);
mean_6_S3 = mean2(im_6_esy_s3_1);
mean_6_S4 = mean2(im_6_esy_s4_1);
mean_6_S5 = mean2(im_6_esy_s5_1);
mean_6_S6 = mean2(im_6_esy_s6_1);
mean_6_S7 = mean2(im_6_esy_s7_1);
mean_6_best = mean ([mean_6_S1,mean_6_S2, mean_6_S3,mean_6_S4, mean_6_S5,
mean_6_S6, mean_6_S7]);
mean_7_S1 = mean2(im_7_esy_s1_1);
mean_7_S2 = mean2(im_7_esy_s2_1);
```

```
mean_7_S3 = mean2(im_7_esy_s3_1);

mean_7_S4 = mean2(im_7_esy_s4_1);

mean_7_S5 = mean2(im_7_esy_s5_1);

mean_7_S6 = mean2(im_7_esy_s6_1);

mean_7_S7 = mean2(im_7_esy_s7_1);

mean_7_best = mean ([mean_7_S1,mean_7_S2, mean_7_S3,mean_7_S4, mean_7_S5,

mean_7_S6, mean_7_S7]);

mean_8_S1 = mean2(im_8_esy_s1_1);

mean_8_S2 = mean2(im_8_esy_s2_1);

mean_8_S3 = mean2(im_8_esy_s3_1);

mean_8_S4 = mean2(im_8_esy_s4_1);

mean_8_S5 = mean2(im_8_esy_s5_1);

mean_8_S6 = mean2(im_8_esy_s6_1);

mean_8_S7 = mean2(im_8_esy_s7_1);

mean_8_best = mean ([mean_8_S1,mean_8_S2, mean_8_S3,mean_8_S4, mean_8_S5,

mean_8_S6, mean_8_S7]);

mean_10_S1 = mean2(im_10_esy_s1_1);

mean_10_S2 = mean2(im_10_esy_s2_1);

mean_10_S3 = mean2(im_10_esy_s3_1);

mean_10_S4 = mean2(im_10_esy_s4_1);

mean_10_S5 = mean2(im_10_esy_s5_1);

mean_10_S6 = mean2(im_10_esy_s6_1);

mean_10_S7 = mean2(im_10_esy_s7_1);
```

```
mean_10_best = mean ([mean_10_S1,mean_10_S2, mean_10_S3,mean_10_S4,
mean_10_S5, mean_10_S6, mean_10_S7]);
mean_12_S1 = mean2(im_12_esy_s1_1);
mean_12_S2 = mean2(im_12_esy_s2_1);
mean_12_S3 = mean2(im_12_esy_s3_1);
mean_12_S4 = mean2(im_12_esy_s4_1);
mean_12_S5 = mean2(im_12_esy_s5_1);
mean_12_S6 = mean2(im_12_esy_s6_1);
mean_12_S7 = mean2(im_12_esy_s7_1);
mean_12_best = mean ([mean_12_S1,mean_12_S2, mean_12_S3,mean_12_S4,
mean_12_S5, mean_12_S6, mean_12_S7]);
% plot result
%Array of average pixel value of all concentrations (Y-axis)
avg_pixel_S1=[ mean_2_S1,  mean_4_S1, mean_6_S1, mean_7_S1,
mean_8_S1,  mean_10_S1, mean_12_S1];
avg_pixel_S2=[ mean_2_S2,  mean_4_S2, mean_6_S2, mean_7_S2,
mean_8_S2,  mean_10_S2, mean_12_S2];
avg_pixel_S3=[ mean_2_S3,  mean_4_S3, mean_6_S3, mean_7_S3,
mean_8_S3,  mean_10_S3, mean_12_S3];
avg_pixel_S4=[ mean_2_S4,  mean_4_S4, mean_6_S4, mean_7_S4,
mean_8_S4,  mean_10_S4, mean_12_S4];
avg_pixel_S5=[ mean_2_S5,  mean_4_S5, mean_6_S5, mean_7_S5,
mean_8_S5,  mean_10_S5, mean_12_S5];
```

```
avg_pixel_S6=[ mean_2_S6,  mean_4_S6, mean_6_S6, mean_7_S6,
mean_8_S6,  mean_10_S6, mean_12_S6];
avg_pixel_S7=[ mean_2_S7,  mean_4_S7, mean_6_S7, mean_7_S7,
mean_8_S7,  mean_10_S7, mean_12_S7];
avg_pixel_best = [ mean_2_best,  mean_4_best, mean_6_best,
mean_7_best,mean_8_best, mean_10_best,mean_12_best];
%Array of selected pH level (X-axis)
ph_value=[ 2 4 6 7 8 10 12];
figure();
pH_plot=plot(ph_value, avg_pixel_S1,'b--*',ph_value, avg_pixel_S2,'g--*', ph_value,
avg_pixel_S3,'r--*',ph_value, avg_pixel_S4,'c--*',ph_value, avg_pixel_S5,'m--*',
ph_value, avg_pixel_S6,'y--*', ph_value, avg_pixel_S7,'k--*');
%Standardizing range of Y axis
axis([2 14 90 160])
title('pH vs. Intensity (Red BPF, Red LED)');
xlabel('pH Level');
ylabel('Intensity');
legend('Sample 1','Sample 2','Sample 3','Sample 4','Sample 5','Sample 6','Sample
7','Mean');
legend('Location','northeast');
%Standard Deviation calculation using errorbar function
x = [avg_pixel_S1 ; avg_pixel_S2; avg_pixel_S3;avg_pixel_S4 ; avg_pixel_S5;
avg_pixel_S6;avg_pixel_S7];
```

```
y = ph_value;

e = std(x,0,1);

figure();

errorbar(y,avg_pixel_best,e);

axis([0 14 90 160])

title('Error Bar (Red BPF, Red LED)');

xlabel('pH Level');

ylabel('Intensity');
```

APPENDIX C

MATLAB CODE (M-FILE) FOR RGB ANALYSIS

The MATLAB m- file to produce figure 10 (b) in paper II as follows:

```
clc; clear; close all;
% read and crop pH2, pH4, pH6, pH7, pH8, pH10, pH12 strip color images.
crop_area = [180 140 920 582];
%pH2 crop
pH2rgb1 = imread('pH2_n_1.BMP');
pH2croprgb1=imcrop(pH2rgb1,crop_area);
pH2rgb2 = imread('pH2_n_2.BMP');
pH2croprgb2=imcrop(pH2rgb2,crop_area);
pH2rgb3 = imread('pH2_n_3.BMP');
pH2croprgb3=imcrop(pH2rgb3,crop_area);
%pH4 crop
pH4rgb1 = imread('pH4_n_1.BMP');
pH4croprgb1=imcrop(pH4rgb1,crop_area);
pH4rgb2 = imread('pH4_n_2.BMP');
pH4croprgb2=imcrop(pH4rgb2,crop_area);
pH4rgb3 = imread('pH4_n_3.BMP');
pH4croprgb3=imcrop(pH4rgb3,crop_area);
%Repeat the above image reading steps for pH6, pH7, pH8, pH10, pH12
%Break R,G,B frames
%break pH2
pH2RFrame1 = pH2croprgb1(:,:,1);
```

```
pH2GFrame1 = pH2croprgb1(:,:,2);

pH2BFrame1 = pH2croprgb1(:,:,3);

pH2RFrame2 = pH2croprgb2(:,:,1);

pH2GFrame2 = pH2croprgb2(:,:,2);

pH2BFrame2 = pH2croprgb2(:,:,3);

pH2RFrame3 = pH2croprgb3(:,:,1);

pH2GFrame3 = pH2croprgb3(:,:,2);

pH2BFrame3 = pH2croprgb3(:,:,3);

%break pH4

pH4RFrame1 = pH4croprgb1(:,:,1);

pH4GFrame1 = pH4croprgb1(:,:,2);

pH4BFrame1 = pH4croprgb1(:,:,3);

pH4RFrame2 = pH4croprgb2(:,:,1);

pH4GFrame2 = pH4croprgb2(:,:,2);

pH4BFrame2 = pH4croprgb2(:,:,3);

pH4RFrame3 = pH4croprgb3(:,:,1);

pH4GFrame3 = pH4croprgb3(:,:,2);

pH4BFrame3 = pH4croprgb3(:,:,3);

%Repeat the above steps for splitting RGB data in three different array for pH6, pH7,

pH8, pH10, pH12

%Finding the desired RGB intensities from R,G,B frames of each  pH strip image

%pH 2

pH2RMax1 = max(max(pH2RFrame1));
```

```
pH2GMax1 = min(min(pH2GFrame1));
pH2BMax1 = min(min(pH2BFrame1));
pH2RMax2 = max(max(pH2RFrame2));
pH2GMax2 = min(min(pH2GFrame2));
pH2BMax2 = min(min(pH2BFrame2));
pH2RMax3 = max(max(pH2RFrame3));
pH2GMax3 = min(min(pH2GFrame3));
pH2BMax3 = min(min(pH2BFrame3));
%pH4
pH4RMax1 = max(max(pH4RFrame1));
pH4GMax1 = min(min(pH4GFrame1));
pH4BMax1 = min(min(pH4BFrame1));
pH4RMax2 = max(max(pH4RFrame2));
pH4GMax2 = min(min(pH4GFrame2));
pH4BMax2 = min(min(pH4BFrame2));
pH4RMax3 = max(max(pH4RFrame3));
pH4GMax3 = min(min(pH4GFrame3));
pH4BMax3 = min(min(pH4BFrame3));
%pH6
pH6RMax1 = max(max(pH6RFrame1));
pH6GMax1 = max(max(pH6GFrame1));
pH6BMax1 = min(min(pH6BFrame1));
pH6RMax2 = max(max(pH6RFrame2));
```

```
pH6GMax2 = max(max(pH6GFrame2));
pH6BMax2 = min(min(pH6BFrame2));
pH6RMax3 = max(max(pH6RFrame3));
pH6GMax3 = max(max(pH6GFrame3));
pH6BMax3 = min(min(pH6BFrame3));
%pH7
pH7RMax1 = min(min(pH7RFrame1));
pH7GMax1 = max(max(pH7GFrame1));
pH7BMax1 = min(min(pH7BFrame1));
pH7RMax2 = min(min(pH7RFrame2));
pH7GMax2 = max(max(pH7GFrame2));
pH7BMax2 = min(min(pH7BFrame2));
pH7RMax3 = min(min(pH7RFrame3));
pH7GMax3 = max(max(pH7GFrame3));
pH7BMax3 = min(min(pH7BFrame3));
%pH8
pH8RMax1 = min(min(pH8RFrame1));
pH8GMax1 = max(max(pH8GFrame1));
pH8BMax1 = min(min(pH8BFrame1));
pH8RMax2 = min(min(pH8RFrame2));
pH8GMax2 = max(max(pH8GFrame2));
pH8BMax2 = min(min(pH8BFrame2));
pH8RMax3 = min(min(pH8RFrame3));
```

```
pH8GMax3 = max(max(pH8GFrame3));

pH8BMax3 = min(min(pH8BFrame3));

%pH10

pH10RMax1 = min(min(pH10RFrame1));

pH10GMax1 = mean(mean(pH10GFrame1));

pH10BMax1 = max(max(pH10BFrame1));

pH10RMax2 = min(min(pH10RFrame2));

pH10GMax2 = mean(mean(pH10GFrame2));

pH10BMax2 = max(max(pH10BFrame2));

pH10RMax3 = min(min(pH10RFrame3));

pH10GMax3 = mean(mean(pH10GFrame3));

pH10BMax3 = max(max(pH10BFrame3));

%pH12

pH12RMax1 = min(min(pH12RFrame1));

pH12GMax1 = min(mean(pH12GFrame1));

pH12BMax1 = max(max(pH12BFrame1));

pH12RMax2 = min(min(pH12RFrame2));

pH12GMax2 = min(mean(pH12GFrame2));

pH12BMax2 = max(max(pH12BFrame2));

pH12RMax3 = min(min(pH12RFrame3));

pH12GMax3 = min(mean(pH12GFrame3));

pH12BMax3 = max(max(pH12BFrame3));

%Max of R,G,B frames
```

```
pH2RMax = max([pH2RMax1 pH2RMax2 pH2RMax3]);
pH2GMax = min([pH2GMax1 pH2GMax2 pH2GMax3]);
pH2BMax = min([pH2BMax1 pH2BMax2 pH2BMax3]);
pH4RMax = max([pH4RMax1 pH4RMax2 pH4RMax3]);
pH4GMax = min([pH4GMax1 pH4GMax2 pH4GMax3]);
pH4BMax = min([pH4BMax1 pH4BMax2 pH4BMax3]);
pH6RMax = max([pH6RMax1 pH6RMax2 pH6RMax3]);
pH6GMax = min([pH6GMax1 pH6GMax2 pH6GMax3]);
pH6BMax = min([pH6BMax1 pH6BMax2 pH6BMax3]);
pH7RMax = min([pH7RMax1 pH7RMax2 pH7RMax3]);
pH7GMax = max([pH7GMax1 pH7GMax2 pH7GMax3]);
pH7BMax = min([pH7BMax1 pH7BMax2 pH7BMax3]);
pH8RMax = min([pH8RMax1 pH8RMax2 pH8RMax3]);
pH8GMax = max([pH8GMax1 pH8GMax2 pH8GMax3]);
pH8BMax = min([pH8BMax1 pH8BMax2 pH8BMax3]);
pH10RMax = min([pH10RMax1 pH10RMax2 pH10RMax3]);
pH10GMax = mean([pH10GMax1 pH10GMax2 pH10GMax3]);
pH10BMax = max([pH10BMax1 pH10BMax2 pH10BMax3]);
pH12RMax = min([pH12RMax1 pH12RMax2 pH12RMax3]);
pH12GMax = min([pH12GMax1 pH12GMax2 pH12GMax3]);
pH12BMax = max([pH12BMax1 pH12BMax2 pH12BMax3]);
%Convert max of RGB to XYZ
%copy structure
```

```
pH2croprgb = pH2croprgb1;

pH4croprgb = pH4croprgb1;

%Repeat the above steps for pH6, pH7, pH8, pH10, pH12


%insert data

pH2croprgb(:,:,1) = pH2RMax;

pH2croprgb(:,:,2) = pH2GMax;

pH2croprgb(:,:,3) = pH2BMax;

pH4croprgb(:,:,1) = pH4RMax;

pH4croprgb(:,:,2) = pH4GMax;

pH4croprgb(:,:,3) = pH4BMax;

%Repeat the above steps for pH6, pH7, pH8, pH10, pH12

pH2_rgb_r_1 = max(max(pH2RFrame1));

pH2_rgb_g_1 = mean(mean(pH2GFrame1));

pH2_rgb_b_1 = mean(mean(pH2BFrame1));

pH2_rgb_r_2 = max(max(pH2RFrame2));

pH2_rgb_g_2 = mean(mean(pH2GFrame2));

pH2_rgb_b_2 = mean(mean(pH2BFrame2));

pH2_rgb_r_3 = max(max(pH2RFrame3));

pH2_rgb_g_3 = mean(mean(pH2GFrame3));

pH2_rgb_b_3 = mean(mean(pH2BFrame3));

pH2_rgb_r = mean([max(max(pH2RFrame1)) max(max(pH2RFrame2))

max(max(pH2RFrame3))]);
```

```
pH2_rgb_g = mean([mean(mean(pH2GFrame1)) mean(mean(pH2GFrame2))
mean(mean(pH2GFrame3))]);
pH2_rgb_b = mean([mean(mean(pH2BFrame1)) mean(mean(pH2BFrame2))
mean(mean(pH2BFrame3))]);
pH4_rgb_r_1 = max(max(pH4RFrame1));
pH4_rgb_g_1 = mean(mean(pH4GFrame1));
pH4_rgb_b_1 = mean(mean(pH4BFrame1));
pH4_rgb_r_2 = max(max(pH4RFrame2));
pH4_rgb_g_2 = mean(mean(pH4GFrame2));
pH4_rgb_b_2 = mean(mean(pH4BFrame2));
pH4_rgb_r_3 = max(max(pH4RFrame3));
pH4_rgb_g_3 = mean(mean(pH4GFrame3));
pH4_rgb_b_3 = mean(mean(pH4BFrame3));
pH4_rgb_r = mean([max(max(pH4RFrame1)) max(max(pH4RFrame2))
max(max(pH4RFrame3))]);
pH4_rgb_g = mean([mean(mean(pH4GFrame1)) mean(mean(pH4GFrame2))
mean(mean(pH4GFrame3))]);
pH4_rgb_b = mean([mean(mean(pH4BFrame1)) mean(mean(pH4BFrame2))
mean(mean(pH4BFrame3))]);
pH6_rgb_r_1 = mean(mean(pH6RFrame1));
pH6_rgb_g_1 = mean(mean(pH6GFrame1));
pH6_rgb_b_1 = mean(mean(pH6BFrame1));
pH6_rgb_r_2 = mean(mean(pH6RFrame2));
```

```
pH6_rgb_g_2 = mean(mean(pH6GFrame2));
pH6_rgb_b_2 = mean(mean(pH6BFrame2));
pH6_rgb_r_3 = mean(mean(pH6RFrame3));
pH6_rgb_g_3 = mean(mean(pH6GFrame3));
pH6_rgb_b_3 = mean(mean(pH6BFrame3));
pH6_rgb_r = mean([mean(mean(pH6RFrame1)) mean(mean(pH6RFrame2))
mean(mean(pH6RFrame3))]);
pH6_rgb_g = mean([mean(mean(pH6GFrame1)) mean(mean(pH6GFrame2))
mean(mean(pH6GFrame3))]);
pH6_rgb_b = mean([mean(mean(pH6BFrame1)) mean(mean(pH6BFrame2))
mean(mean(pH6BFrame3))]);
%Repeat the pH6 steps for pH7, pH8, pH10, pH12
%Sample 1
y_r_1 = [pH2_rgb_r_1, pH4_rgb_r_1, pH6_rgb_r_1, pH7_rgb_r_1,
pH8_rgb_r_1,pH10_rgb_r_1,pH12_rgb_r_1];
y_g_1 = [pH2_rgb_g_1, pH4_rgb_g_1, pH6_rgb_g_1, pH7_rgb_g_1,
pH8_rgb_g_1,pH10_rgb_g_1,pH12_rgb_g_1];
y_b_1 = [pH2_rgb_b_1, pH4_rgb_b_1, pH6_rgb_b_1, pH7_rgb_b_1,
pH8_rgb_b_1,pH10_rgb_b_1,pH12_rgb_b_1];
%Sample 2
y_r_2 = [pH2_rgb_r_2, pH4_rgb_r_2, pH6_rgb_r_2, pH7_rgb_r_2,
pH8_rgb_r_2,pH10_rgb_r_2,pH12_rgb_r_2];
```

```
y_g_2 = [pH2_rgb_g_2, pH4_rgb_g_2, pH6_rgb_g_2, pH7_rgb_g_2,
pH8_rgb_g_2,pH10_rgb_g_2,pH12_rgb_g_2];
y_b_2 = [pH2_rgb_b_2, pH4_rgb_b_2, pH6_rgb_b_2, pH7_rgb_b_2,
pH8_rgb_b_2,pH10_rgb_b_2,pH12_rgb_b_2];
%Sample 3
y_r_3 = [pH2_rgb_r_3, pH4_rgb_r_3, pH6_rgb_r_3, pH7_rgb_r_3,
pH8_rgb_r_3,pH10_rgb_r_3,pH12_rgb_r_3];
y_g_3 = [pH2_rgb_g_3, pH4_rgb_g_3, pH6_rgb_g_3, pH7_rgb_g_3,
pH8_rgb_g_3,pH10_rgb_g_3,pH12_rgb_g_3];
y_b_3 = [pH2_rgb_b_3, pH4_rgb_b_3, pH6_rgb_b_3, pH7_rgb_b_3,
pH8_rgb_b_3,pH10_rgb_b_3,pH12_rgb_b_3];
%Mean of all three samples
y_r = [pH2_rgb_r, pH4_rgb_r, pH6_rgb_r, pH7_rgb_r,
pH8_rgb_r,pH10_rgb_r,pH12_rgb_r];
y_g = [pH2_rgb_g, pH4_rgb_g, pH6_rgb_g, pH7_rgb_g,
pH8_rgb_g,pH10_rgb_g,pH12_rgb_g];
y_b = [pH2_rgb_b, pH4_rgb_b, pH6_rgb_b, pH7_rgb_b,
pH8_rgb_b,pH10_rgb_b,pH12_rgb_b];
x_pH = [2 4 6 7 8 10 12];
figure
plot(x_pH, y_r, '-or',x_pH, y_g, '-og',x_pH, y_b, '-ob',x_pH, y_r_1, '-.*r',x_pH, y_r_2, '--
*r',x_pH, y_r_3, ':*r',x_pH, y_g_1, '-.*g',x_pH, y_g_2, '--*g',x_pH, y_g_3, ':*g',x_pH,
y_b_1, '-.*b',x_pH, y_b_2, '--*b',x_pH, y_b_3, ':*b');
```

```
legend('Red','Green','Blue','Location','north')

title('pH Level vs Intensity (No. of Samples = 3)')

xlabel('pH level')

ylabel('Intensity')
```

VITA

Altamash Mukhtar Fakki was born in Navi Mumbai, Maharashtra. He completed his Bachelor of Engineering in Electronics and Telecommunication from Mahatma Gandhi Mission's College of Engineering and Technology affiliated to Mumbai University, Navi Mumbai in September 2010. After his undergrad, Altamash worked as a Software Engineer for 2 years and 10 months at Mastek Limited, India. Because of his interest in sensors, embedded systems and programming, Altamash started his Master of Science in Computer Engineering in August 2013. He did his summer internship with Asynchrony in Summer 2014. He received his masters in May 2015. He worked as a research assistant on biosensor project at Intelligent Microsystem Laboratory under Dr. Chang-Soo Kim. He is taking a Software Engineer position in Cerner Corporation, Kansas City, Missouri, starting in June 2015.